17th International Conference on Space Operations, Dubai, United Arab Emirates, 6 - 10 March 2023.

SpaceOps-2023, ID 396

Reconfigurable satellite constellations: optimal design and maneuvering

Federica Paganelli Azza*, Pietro De Marchi† and Matteo Stoisa‡,
AIKO S.r.l., Via Dei Mille 22, 10123, Torino, Italy

The ability to adapt space systems' geometry to changing mission requirements and unexpected challenges is becoming increasingly important for the future of space exploration. One potential solution is the use of reconfigurable constellations, which allow for active adjustments of the configuration to meet future needs and focus resources towards dynamic objectives. This research introduces a low-thrust reconfiguration strategy based on a multi-objective Genetic Algorithm to optimize these constellations by balancing the trade-off between observation performance over a target area and the cost of reaching the new pattern. The proposed solution is validated in a Low Earth Orbit scenario, specifically reconfiguring from global coverage to regional coverage. The results are compared to those in previous literature to demonstrate the effectiveness of the proposed solution.

I. Introduction

The modern space race has seen an increase in the number of satellite constellations being inserted into Low Earth Orbit (LEO). While large constellations are typically the domain of big players in the industry, smaller and medium-sized constellations are becoming more achievable for both public and private operators. These constellations are commonly used for ground monitoring and telecommunications, but observation missions are the most frequent. While many of these satellites lacked a propulsive subsystem in the past, electric propulsion is opening up the possibility for more satellites to have this capability. Maneuvering satellites offer the opportunity to maintain performance for a constellation and also, to intentionally modify them to achieve different objectives over their lifetime. This allows, for instance, a reconfiguration of the constellation when one or more satellites have failed or the optimal insertion of new satellites into an existing system. The ability to adapt a constellation's geometry in response to changes in the region of interest is also critical for several applications.

While reconfiguration has not been implemented yet in any space mission it has recently been investigated by several research groups, such as deWeck's [1–3], Mortari's [4] and Ferringer's [5]. The concept of a reconfigurable satellite constellation (ReCon) has been proposed [6] as a design strategy to enable a two-mode observation constellation that switches between a Global Observation Mode (GOM) and a Regional Observation Mode (ROM) for contingency responses.

This research extends the results presented in [7] and investigates an optimization framework for the optimal reconfiguration of LEO constellations. The reconfiguration problem is formulated as a multi-objective optimization in which a trade-off between observation performance and the cost of reconfiguration maneuvers is evaluated while considering constraints on available resources. The main focus of the use cases presented in this paper is observing a specific target, such as during ground index monitoring missions. The proposed scenarios consider reconfiguration from a reference geometry to illustrate better the advantages introduced by the parametric optimization. However, the framework is extendable to any combination of starting and arrival geometries, as dictated by changing mission objectives.

Improvements to the framework are ongoing, including a more detailed model of the transfer between orbits for each satellite of the constellation, considering the time of flight, optimal possible transfer, and related consumption. These parameters will become part of the optimization criteria to better assess the real cost of the whole reconfiguration. The framework will also be applied to different scenarios, such as collision avoidance. Optimal reconfiguration in case of

*Corresponding author, federica@aikospace.com
†pietro@aikospace.com
‡matteo@aikospace.com

mandatory maneuvers due to close approaches with other spacecrafts or debris will be increasingly important in the upcoming years due to the impact of constellations on LEO overcrowding.

The paper is organized as follows. First of all, an overview of the physical and geometrical models for evaluating constellation performance and estimating maneuver costs is provided. After that, a section dedicated to the implemented optimization technique is included, describing the main choices behind it. Lastly, the main results of the key use cases are shown, highlighting the capabilities of the algorithm and its flexibility.

II. Physical model

A. Target area model

The overall Earth surface is divided into several tiles of near-equal area as described in [8]. By placing a target point on each tile's centroid, it is possible to obtain sites that are uniformly distributed all over the globe as depicted in Fig. 1. The tessellation algorithm determines each tile's dimensions depending on the payload specifications. In particular, the Field of View (FoV) of the instrument is a critical parameter to compute the sites grid, as the size of each tile should be chosen to ensure that at least one tile is entirely within the FoV of all the satellites in the constellation. Starting from the produced Earth grid, target points are defined according to the Region Of Interest (ROI) given by the user. The desired ROI is specified in terms of its latitude and longitude coordinates and used to identify the target sites.

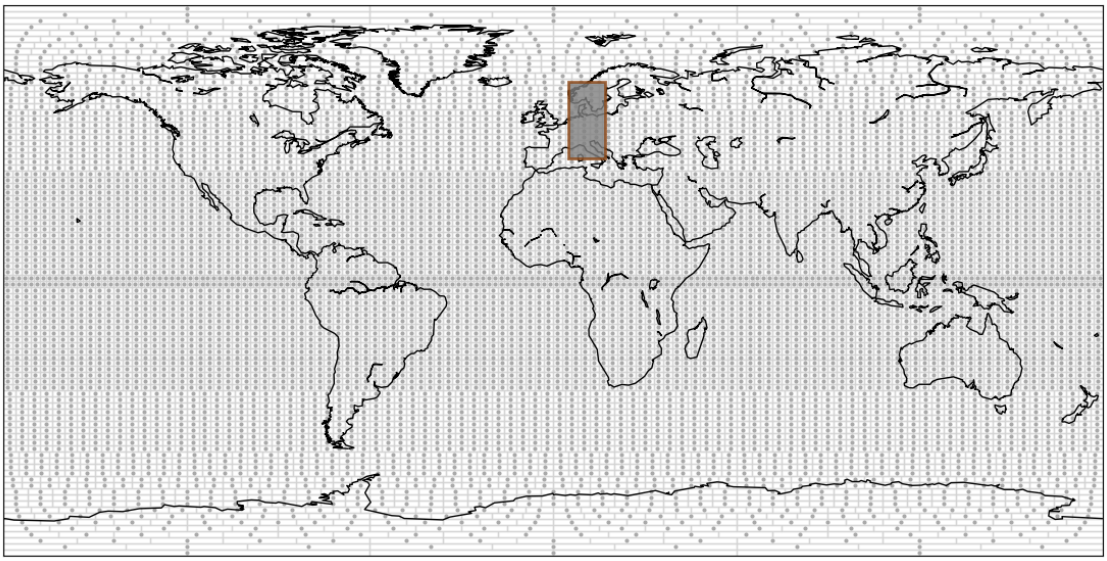

Fig. 1 Target sites for a FoV of 20 degrees and ROI in central Europe.

B. Orbit description and propagation

Each satellite in the constellation is modeled through the keplerian set of orbital parameters. Therefore, six different variables are used to describe a single orbit, that are the semi-major axis a, the eccentricity e, the inclination i, the right ascension of the ascending node Ω, the argument of periapsis ω and the true anomaly ν. A payload with circular FoV is assumed, and the swath length L is retrieved from the spherical Earth approximation [9] as:

$$L = R_E \tan \lambda \tag{1}$$

where R_E is the Earth radius and λ is the Earth central angle.

The choice of the propagation algorithm for satellites' position and velocity is critical when an optimization process is considered. The orbit propagation method affects the optimization routine in two different ways, having impacts on both the quality and the execution time of the overall process.

The models included in the orbit propagator could be more or less precise, providing different accuracy levels to the analysis, and impacting the reliability of the final results. In order to ensure a proper trade-off between computational load

and accuracy, the propagation model employed in the implemented reconfiguration strategy includes the gravitational field and atmospheric drag. This is coherent with the fact that only LEO orbits are considered and the maximum propagation horizon is around ten days (only short and medium term perturbations are relevant). However, the quality of the results is determined also by the adopted propagation type. Special perturbation techniques (or numerical methods) allow more precise orbit determination (depending on the accuracy) while general perturbation methods (or analytical approaches) are generally faster but less accurate. This introduces the second relevant impact of the propagation method on the optimization procedure, as the choice of a more complex model and/or tool could significantly increase the computational times.

Since a proper trade-off between desired accuracy of the final solution and execution time of the propagation has to be enforced, three different propagators have been tested inside the optimization procedure to select the most suitable for the considered use case. In particular, the following tools have been analyzed in terms of delivered accuracy and required computational load:

1) The Basilisk Astrodynamics Framework [10], in which the propagation is performed with a numerical Runge-Kutta-Fehlberg (RKF45) variable step integrator and the gravitational field is described according to the GGM03S model [11].
2) An optimized numerical propagator (Fast-Num), a revisitation of the Hypernova propagator [12] (designed by University of Toronto for the FINCH mission), including J2 and drag (exponential atmosphere) contributions.
3) The HANDE analytical propagator [13], developed from the Hoots perturbations analytical theory and accounting for J2 and drag (Jacchia model 1970 [14]) contributions.

The three propagators presented above are available both in Python and C/C++. While the Python code is deemed more suitable for prototyping, the C/C++ implementation is integrated inside the optimization routine due to its lower computational times. Table 1 compares the performance of the three tools, considering an incremental propagation horizon and employing an integration time step of 10 seconds. The accuracy assessment is performed against a high precision orbit propagation (reference here is NASA's GMAT tool [15] with GGM03 gravity model and NRLMSIS atmosphere model) and the RMS distance about cartesian positions in ECI between each propagator and the reference is collected.

Table 1 Performance achievable with the tested propagators.

Tool	1 month horizon	3 months horizon	Accuracy after 1 month
Basilisk	~ 7.591 s	~ 16.562 s	~ 500 km
Fast-Num	~ 0.088 s	~ 0.253 s	~ 310 km
HANDE	~ 3.1 s	~ 10 s	~ 350 km

Fast-Num and HANDE have been finally chosen for the GA algorithm propagation of the satellites. For constellation reconfiguration purposes the present accuracies are sufficient and does not alter significantly the performance detected. Furthermore both HANDE and Fast-Num allow to reduce significantly the computational times, allowing to simulate bigger constellations faster.

C. Low-thrust maneuvers

As already mentioned in Section I, each satellite in the constellation is equipped with a low-thrust propulsion system. Since the purpose of the proposed reconfiguration approach is to optimize the target configuration of the constellation, it is not possible to fix an a-priori final orbit of the transfer or to rely on predefined sets of available maneuvers. To address the reconfiguration problem, a proper maneuvering framework has to be defined and implemented. In particular, the transfer cost to reach a target orbit $[a_T, e_T, i_T, \Omega_T, \omega_T, \nu_T]$ starting from the initial parameters $[a_0, e_0, i_0, \Omega_0, \omega_0, \nu_0]$ has to be estimated. The change in velocity ΔV requested to obtain the desired transfer is used to assess the feasibility of the maneuver with respect to the available resources. To avoid long computation times, an analytical estimation of the ΔV is preferred to a numerical approach, and it is integrated in the optimization routine to guarantee that the produced solutions can actually be reached from the initial orbit.

The maneuvering strategy presented in [16] is adopted and integrated into the optimization procedure. The cost to perform a given orbit transfer is estimated by assuming that the different orbital parameters are changed simultaneously under the effect of the second-order zonal harmonics of the Earth gravitational potential. As already done in [7], changes in true anomaly are not explicitly included in the cost model as the desired in-plane phasing in the target orbit can be achieved through a proper time shift in the scheduling of the maneuvers. The RAAN phasing cost is instead modeled by

assuming a three-phase maneuver aimed at exploiting the natural drift produced by the Earth oblateness [17] to reach the target RAAN shift.

III. Optimization algorithm

A. Problem overview

The proposed reconfiguration strategy employs a multi-objective optimization to address the reconfiguration problem. The main goal is to provide a proper trade-off between the observation performance over the given area of interest and the cost to reconfigure the constellation. The optimization takes as input the initial constellation pattern, the payload FoV, and the region of interest. It computes the best configuration to maximize the time spent observing the target area while minimizing the overall change in velocity ΔV required to maneuver the satellites.

The optimization variables are represented by the keplerian parameters of the final constellation pattern and are reported in Table 2. The lower and upper bounds of each variable should be defined according to the specific use case. The values reported in Table 2 refer to the LEO scenario taken as reference for the simulation results reported in section IV. An important remark regards the definition of a proper range for the eccentricity value which cannot be fixed a-priori but depends on the actual semi-major axis reached during the optimization. To design proper constraints for a LEO orbit, e_{low} and e_{up} should be modeled to guarantee that the following inequalities are respected:

$$\begin{cases} r_p = a(1-e) \geq 6671km \\ r_a = a(1+e) \leq 7393km \end{cases} \tag{2}$$

where r_p, r_a are the radius at the periapsis and apoapsis of the orbit.

Table 2 Optimization variables.

Variable	Size	Bounds
a	N_{planes}	[6778km; 7178km]
e	N_{planes}	$[e_{low}; e_{up}]$
i	N_{planes}	[0°; 90°]
Ω	N_{planes}	[0°; 360°]
ω	N_{planes}	[0°; 360°]
ν	N_{sat}	[0°; 360°]

B. Genetic algorithm

Genetic algorithms (GA) are widely known evolutionary optimization methods that mimic natural selection processes where individuals compete to survive across several generations [18]. A GA-based optimization is chosen to deal with the complexity of the reconfiguration problem and guarantee a trade-off between a set of conflicting objectives. The suitability of this class of algorithms is mainly due to its ability to locate global optimum solutions in a wide range of non-linear problems [19]. The GA integrated into the proposed reconfiguration strategy is implemented in C++ and the main choices behind its structure and development are explained in detail in a previous work [7]. During each evolution step, the GA evaluates a set of candidate constellations that defines the current population so that only the best amongst them are maintained also in the following generation. The optimization routine depicted in Fig. 2 is repeated iteratively until the termination conditions are reached so that the population - initialized with randomly generated values - evolves towards optimal configurations.

As already highlighted in the previous subsection, the purpose of the reconfiguration problem is to optimize a set of conflicting metrics and find a proper trade-off between the observation performance over the ROI and the maneuvering cost. The design of the fitness function is therefore a critical aspect to ensure that the goodness of each candidate solution is assessed accordingly. The multi-objective optimization is built up in the form of a minimization problem where the overall fitness function is composed of five distinct sub-objectives as:

$$J = \min_{x} \sum_{o=1}^{N_o} w_o f_o(x) \tag{3}$$

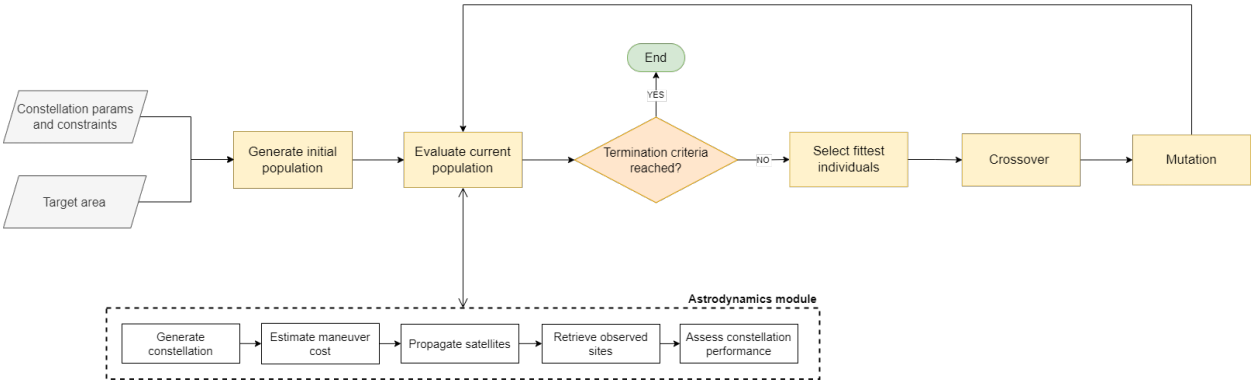

Fig. 2 Genetic Algorithm optimization routine.

where the terms f_o represent the optimization objectives and w_o are the weights used to quantify the importance of the different contributions. Each fitness function f_o is normalized within $[0; 1]$ so that the values of all the contributions are of similar magnitude and the weighted sum approach shown in 3 can be applied. The optimization objectives included in the fitness function and the mathematical approach used to compute them are reported in Table 3. In the notations used for the mathematical expression of each function, subscripts i, k, s represent respectively a specific site, time step, and satellite while N_i, N_k, N_s are the overall number of target sites, propagation steps, and satellites in the constellation. The $coverage\ flag_i$ indicates if a specific target point i in the ROI is observed along the propagation horizon while $coverage_{ik}$ is a boolean value to express if the target i is accessed at time instant k. The maximum available change in velocity for each satellite ΔV_s^{max} can be derived from mission requirements and it is used as a normalization term for the reconfiguration cost contribution while the actual cost of each maneuver ΔV_s is estimated by following the approach described in subsection II.C.

Table 3 Optimization objectives included in the Genetic Algorithm fitness function.

Objective function	Description	Optimization goal	Mathematical formulation
f_1	ROI percentage coverage	Maximization	$1 - \frac{\sum_{i=1}^{N_i} coverage\ flag_i}{N_i}$
f_2	ROI time coverage	Maximization	$1 - \frac{\sum_{i=1}^{N_i} \sum_{k=1}^{N_k} coverage_{ik}}{N_i N_k}$
f_3	ROI maximum revisit time	Minimization	$\frac{\sum_{i=1}^{N_i} max\ revisit_i}{N_i N_k}$
f_4	ROI average revisit time	Minimization	$\frac{\sum_{i=1}^{N_i} revisit_i}{N_i N_k}$
f_5	Reconfiguration cost	Minimization	$\sum_{s=1}^{N_s} \frac{\Delta V_s}{\Delta V_s^{max}}$

C. Parallelization

A critical aspect of the reconfiguration problem is that its complexity poses severe constraints on the efficiency of the optimization procedure and leads to high computational loads. Since the time required to provide the optimal solution is a key feature of a successful reconfiguration strategy, it is important to devise an approach to speed up the computational time. This can be done by exploiting one of the advantages of GAs. The way these algorithms work predisposes them to parallel processing and various parallelization methods can be designed and integrated into their structure [20]. To investigate the impact of a parallel GA, three different implementations of the algorithm have been compared. In particular, concurrent programming has been used to provide a multi-processing architecture and optimize the usage of the available hardware resources [21]. The implementation strategies followed to analyze the computational time required by the GA are:

1) A purely sequential approach (P_A), in which the candidate solutions in each population are evaluated one at a time without any parallel computation.

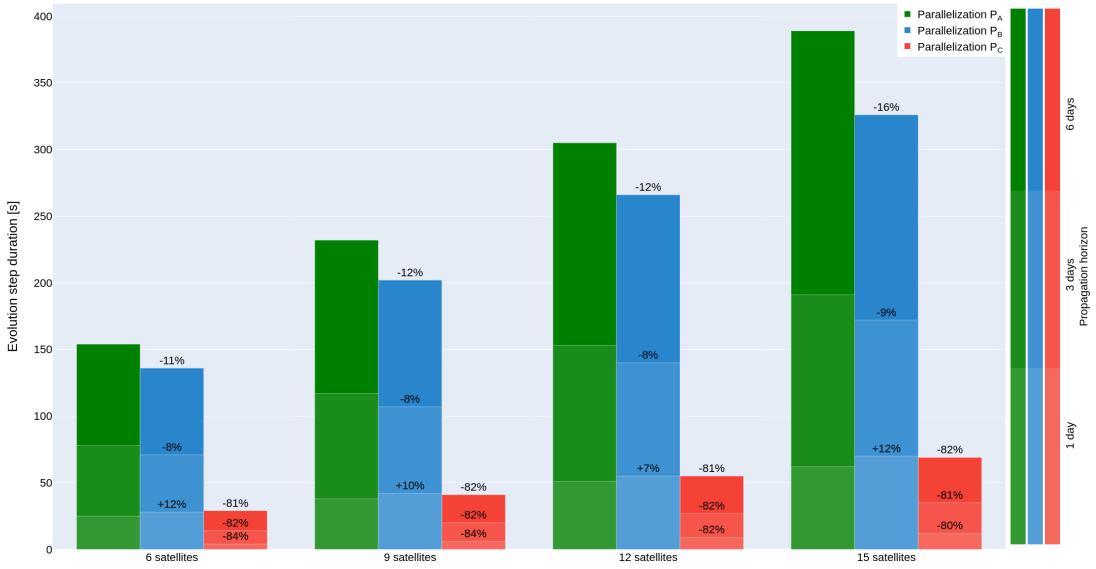

Fig. 3 Computational times reached with parallel implementations of the Genetic Algorithm.

2) A parallel propagation approach (P_B), where the orbital propagation of the satellites belonging to the same candidate constellation configuration is performed in a parallel fashion.
3) A parallel evaluation approach (P_C), that exploits the independence of each candidate solution to the others and implements a fully parallel evaluation of each constellation in the population.

A comparison between the three implementation strategies is available in Fig. 3. A population built with 250 individuals is taken as reference and the times needed to complete an evolution step using a laptop *AMD Ryzen 5 5600U* CPU are reported. To investigate the performance provided in reconfiguration scenarios, the same test is performed considering increasing constellation sizes and propagation horizons.

It is possible to notice that the parallel propagation approach P_B offers slight improvements in case of bigger constellations. This approach strongly depends on the propagation horizon and constellation size, and in general it does not provide satisfactory improvements in the considered scenarios. The parallel evaluation approach P_C is instead able to generalize better as the parallelization degree can be maximized across the available hardware resources having as the upper limit the total number of individuals in each generation. In particular, in the considered testing conditions it is possible to achieve savings in the execution time up to 80% if compared with the purely sequential approach P_A.

IV. Performance analysis

A. Simulation scenario

The implemented reconfiguration strategy is tested in a LEO scenario. A mission that demands a change in its observation requirements is taken as the reference use case for the results presented in this section. In particular, it is assumed that, after a first operational phase in global coverage mode, the constellation configuration has to be optimized to observe a given area of interest. The ROI that drives the reconfiguration is located in central Europe between latitude 40°-65° and longitude 5°-17°. This area is used to identify a set of relevant target points on the Earth's surface by following the procedure described in section II. Each satellite in the constellation hosts an imaging sensor with a circular FoV that has a half-angle of 10.

The initial configuration is fixed and represented by a Walker-δ (64)n/3/2 [22], chosen as a suitable pattern to achieve global coverage. The geometry of the final constellation is instead computed with the GA by optimizing the orbital parameters of its satellites. Simulations are carried out starting from March 23^{rd}, 2020, and a time step of 30 sec is employed to compute the observation metrics. It is important to notice that this time step only refers to the GA

fitness function, which benefits from lower computational loads. However, GA optimization is validated against a more accurate computation of performance metrics that rely on a time step of 10 sec.

To analyze the effect of each parameter on the implemented algorithm, different scenarios are simulated and compared. In particular, three main classes of sensitivity analysis are reported in this section. At first, the length of the propagation horizon is investigated to provide proper selection criteria. Then, the size of the constellation is studied to show how the reconfiguration strategy is impacted by the number of satellites. At last, different weights for the GA fitness contributions are used and their impact on the achievable performance is examined. In the last part of the section, the final results for the reference scenario are presented and evaluated. All the tests reported in this section refer to the execution on 8 cores of a *AMD Threadripper 2990WX* CPU and the GA parameters are set to reach convergence in the optimization routine (200 max generations, population size of 250, elitism equal to 8).

B. Propagation horizon

The length of the propagation horizon employed in the optimization routine strongly affects the quality of the solutions. This parameter should be sized properly to ensure its compatibility with mission requirements and to determine suitable station-keeping strategies for the target pattern. In this subsection, a sensitivity analysis on the propagation horizon value is proposed and the impact that increasing lengths have on the performance of the final solution is investigated. The initial Walker-δ (64)n/3/2 constellations are taken as reference, however, the same conclusions can be generalized also to the GA-based configurations.

Table 4 collects the revisit time performance guaranteed by Walker-δ with an increasing number of satellites considering different values for the propagation horizon (1, 3, 6, 9, 12 days). Maximum and average ROI revisit times have been chosen as representative metrics because they both belong to the optimization objectives and characterize well the constellation performances.

Table 4 Revisit time evolution with increasing propagation time.

Constellation	Revisit performance	1 day horizon	3 days horizon	6 days horizon	9 days horizon	12 days horizon
Walker-δ (64)6/3/2	Max ROI revisit [h]	8.65	15.76	24.53	30.31	33.2
	Average ROI revisit [h]	6.30	9.76	10.41	10.82	10.97
Walker-δ (64)9/3/2	Max ROI revisit [h]	7.77	14.09	18.82	20.55	20.99
	Average ROI revisit [h]	5.27	7.08	7.30	7.40	7.44
Walker-δ (64)12/3/2	Max ROI revisit [h]	7.29	12.22	15.66	17.03	17.89
	Average ROI revisit [h]	4.19	5.27	5.36	5.40	5.42

From the presented results, it is possible to notice that revisit time values converge asymptotically as the propagation horizon increases. The convergence rate is faster with larger constellation sizes - given that the number of planes is kept constant - and the average revisit time shows smaller variations with respect to the maximum revisit time, being more robust than the maximum to statistical variations. Since the length of the overall horizon strongly determines the overall computational time needed for the optimization, a suitable trade-off has been identified in the six days propagation horizon. The results presented in the following subsection are therefore executed assuming this horizon, considered long enough for the convergence of the average revisit time also in case of the smallest constellation size.

C. Constellation size

The implemented reconfiguration strategy is scalable with respect to the number of satellites in the constellation. The performance achievable through the proposed optimization can be analyzed both in terms of computational load and observation metrics guaranteed on the ROI. To investigate the effects of larger constellations, this subsection assumes systems with a number of satellites $n \in N_{sat} = \{6, 9, 12, 15\}$ while the number of planes is fixed to $N_{planes} = 3$. The computational time exhibits a linear trend that grows with an increasing number of satellites in the constellation. This is in accordance with the parallel implementation of the GA presented in subsection III.C. The observation performance achievable on the ROI for a 6 days propagation horizon is instead reported in Table 5 - inside the green cells - and compared with the one guaranteed by the initial Walker-δ (64)n/3/2. Also, the global mean revisit times of the different GA solution are shown in Fig. 4. Since the main purpose of this analysis is to show how the achievable performance metrics change if a larger constellation is adopted, the fitness weights are chosen so as to maximize the observation performance during the GA optimization without an explicit minimization of the reconfiguration cost. An in-depth

analysis on how the fitness weights affect the GA-based configuration is reported in the following subsection.

Table 5 Revisit time of GA-based and Walker-δ configurations with increasing constellation size.

Constellation size	Max ROI revisit time [h]	Average ROI revisit time [h]
6	24.5	10.4
	17.1	6.8
9	18.8	7.3
	13.6	5.1
12	16.1	5.5
	9.4	3.8
15	9.71	4.40
	8.4	2.9

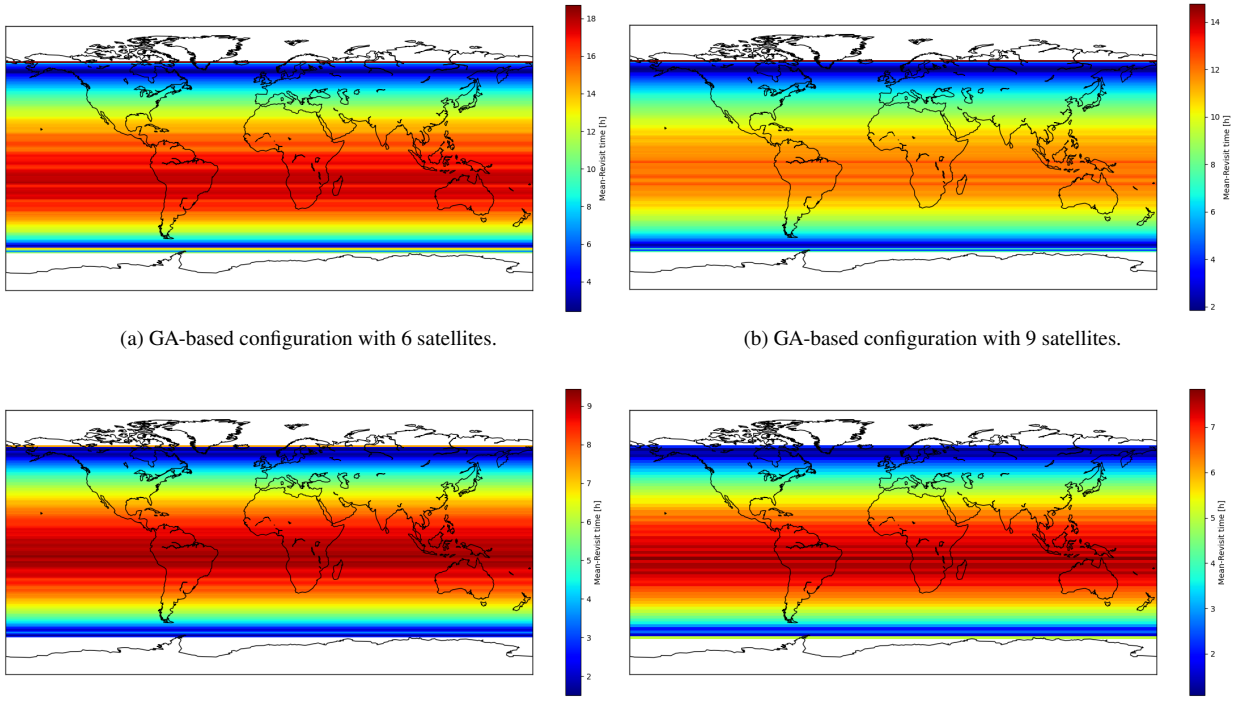

(a) GA-based configuration with 6 satellites.

(b) GA-based configuration with 9 satellites.

(c) GA-based configuration with 12 satellites.

(d) GA-based configuration with 15 satellites.

Fig. 4 Mean revisit times of GA-based configurations of increasing sizes.

D. Fitness weights

As described in subsection III.B, a multi-objective optimization is implemented to assess each solution in terms of both ROI observation performance and reconfiguration cost. Since a weighted sum approach is used in building the overall fitness function, the GA-based configurations depend on the specific set of weights used to balance the five fitness contributions. The quality of the optimization in focusing on the fulfillment of a specific objective can therefore be tuned by setting proper weights inside the fitness function. In this subsection, the impact of different weight configurations are analyzed and compared to show how the proposed strategy can be tailored to specific optimization needs. A constellation of 6 satellites is considered and the GA-based solutions obtained with a propagation horizon of 6 days and different fitness weights are compared. In particular, the following fitness configurations are examined:

1) Unconstrained observation optimization (W_A), characterized by an optimization of the ROI observation performance without any constraint on the reconfiguration cost. In this scenario, the change in velocity needed to perform the reconfiguration is not subject to an upper bound and the weight configuration is given by $W_A = [0.25, 0.25, 0.25, 0.25, 0]$.

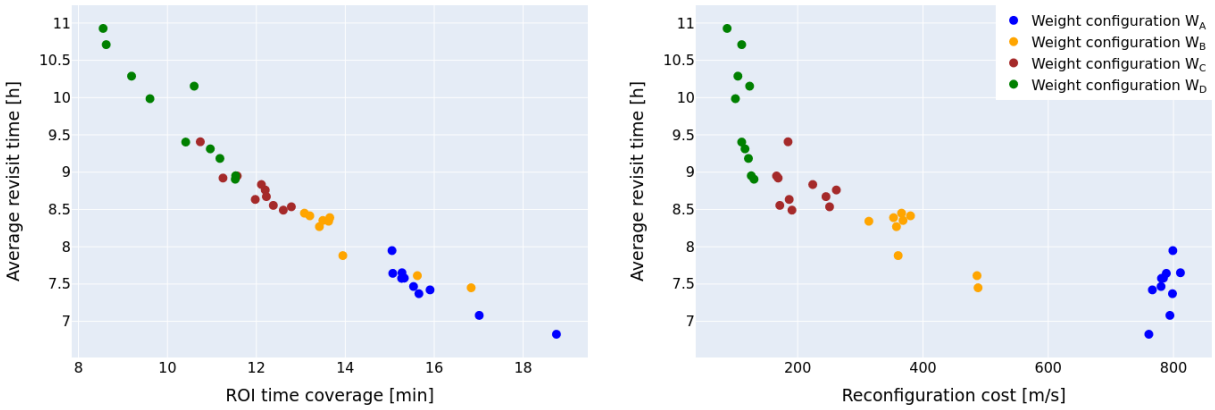

Fig. 5 Effect of different fitness weights configurations.

2) Constrained observation optimization (W_B), that introduces a maximum reconfiguration cost for the optimization. As in the previous configuration, only the ROI observation performance is included explicitly in the fitness function, but a threshold of 500m/s is used to limit the overall cost of the maneuvers. The weight configuration is given by $W_B = [0.25, 0.25, 0.25, 0.25, 0]$.
3) Mid-cost optimization (W_C), where a trade-off between ROI observation and reconfiguration cost should be enforced. The weight configuration is given by $W_C = [0.225, 0.25, 0.25, 0.25, 0.025]$.
4) Low-cost optimization (W_D), that imposes a higher weight for the reconfiguration cost at the expense of lower ROI observations. The weight configuration is $W_D = [0.225, 0.225, 0.225, 0.225, 0.1]$.

The analysis is restricted to the four configurations presented above since they are deemed sufficient to highlight the main trends of the optimization. However, the weight configuration can be freely chosen and the presented results can be generalized, enabling to achieve intermediate solutions.

The results for the weight configurations W_A, W_B, W_C, W_D are presented in Fig. 5 and show how the GA-based solutions are positioned in terms of achievable ROI average revisit time, ROI time coverage and reconfiguration cost. As expected, the minimization of the reconfiguration cost conflicts with the maximization of the ROI observation performance, and the GA solutions are placed on a Pareto front of equally optimal solutions that could be discriminated only with respect to the specific mission requirements. By correctly sizing the maximum reconfiguration cost allowed for each scenario, it is, therefore, possible to pick the best solutions that guarantee the satisfaction of the requirements.

E. Performance analysis

This subsection presents an overview of achievable performance with the proposed reconfiguration strategy. The simulation scenario described above is assumed and results obtained with an increasing constellation size and a fixed propagation horizon of 6 days are shown in Table 6. The performance is analyzed in terms of the optimization objectives introduced in subsection III.B, considering both the ROI observations and the reconfiguration cost. Data are collected for all four different fitness weight configurations described in the previous subsection to highlight how the results are affected by the chosen trade-off between cost and observation. Also, the advantages offered by the GA-based configurations with respect to the corresponding Walker-δ patterns are reported in the green cells. It is possible to notice that the GA-based configurations are able to improve the respective Walker-δ in all the test cases. This advantage seems to be more evident when the size of the constellation is smaller, as the final asymmetrical pattern is able to better mitigate the inevitable longer intervals between ROI observations achieved with a symmetrical configuration. An important notice is that this increased performance does not correspond to a higher average change in velocity with respect to the ones needed with larger constellations. As expected, when the transfer cost is given a higher weight, the observation performance is slightly decreased.

Up to now, a free optimization of the target pattern has been investigated to show the advantages that asymmetrical objective-oriented geometries could offer. However, a desired target configuration can be enforced through properly defined constraints between the orbital parameters of the GA-based solution. This could be exploited to obtain predefined

geometries such as Repeating Ground Track (RGT) orbits. These geometries are commonly used for regional or specific target observations as they offer enhanced partial coverage properties while being easy to design [1]. The results presented above could be therefore expanded by including RGT orbits in the analysis as proper benchmarks for the GA-based solutions, as already done in [7]. The global and local revisit time performance guaranteed by the Walker-δ, the optimized RGT, and the GA-based configurations for a constellation of 12 satellites are compared in Fig. 6. Both the RGT and the GA-based patterns are produced considering the fitness weight configuration W_C introduced in subsection IV.D. It can be noticed that the GA-based configuration is able to achieve enhanced observations of the ROI with respect to the RGT pattern, as the free optimization of the geometry could better exploit the available satellites and focus them toward the objectives.

Table 6 Test cases and achieved performance with a 6-days propagation horizon.

Constellation size	GA runtime [h]	Fitness weights configuration	ROI observation time [min]	Max ROI revisit time [h]	Average ROI revisit time [h]	Reconfiguration cost [m/s]
6	2	A	18.7	17.1 -30.3%	6.8 -34.6%	799
		B	16.8	17.7 -30.2%	7.4 -28.8%	487
		C	11.6	20.7 -15.5%	8.9 -14.4%	166
		D	11.5	20.8 -15.1%	9.1 -12.5%	130
9	3	A	23.6	13.6 -27.7%	5.1 -30.1%	724
		B	19.9	13.9 -26%	5.7 -21.9%	355
		C	17.9	15.3 -18.6%	5.8 -20.5%	148
		D	14.9	15.9 -15.4%	6.7 -8.2%	101
12	4	A	31.3	9.4 -41.6%	3.8 -30.9%	604
		B	27.9	9.8 -39.1%	4.1 -25.5%	366
		C	23.5	10.2 -36.6%	4.5 -18.2%	151
		D	19.1	12.5 -22.4%	5.0 -9.1%	100
15	5	A	42.1	8.4 -13.5%	2.9 -34.1%	661
		B	36.8	8.6 -11.4%	3.3 -25%	361
		C	27.7	9.5 -2.1%	3.8 -13.6%	129
		D	23.2	9.6 -1.1%	4.2 -4.5%	109

V. Conclusions and next steps

The proposed reconfiguration algorithm is capable of achieving an optimized constellation geometry when a specific area of interest or mission objective related to an Earth observation mission is provided. In this research, the reconfiguration performance is demonstrated using the Walker pattern as an example, but the algorithm can be applied to any initial constellation of any size. This flexibility enables the framework to be adapted to various objectives, such as monitoring ground indexes, commercial observation, or institutional missions, and also allows for multiple reconfiguration purposes. Reconfiguration may be necessary to adapt to changing mission objectives, as well as to reach

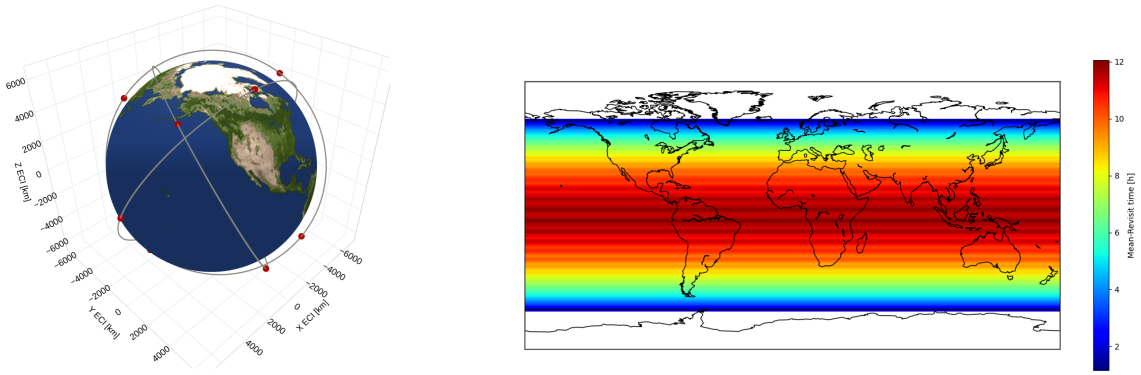

(a) Walker-δ configuration with 12 satellites.

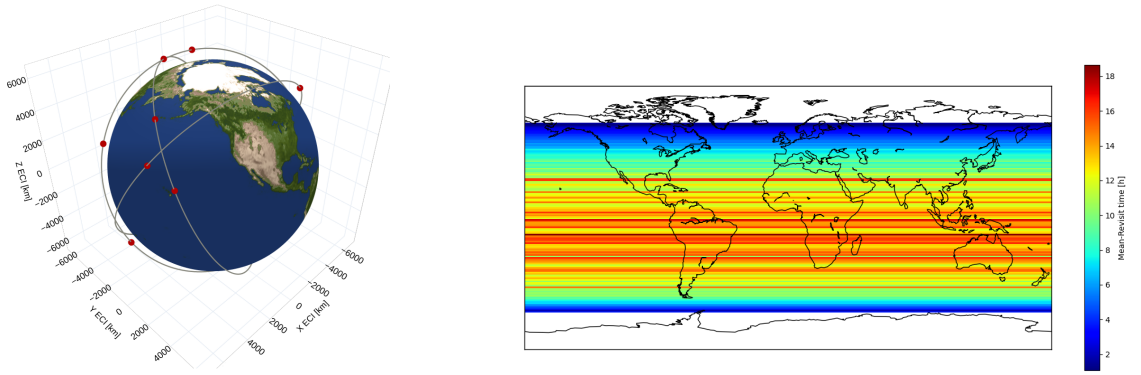

(b) RGT configuration with 12 satellites.

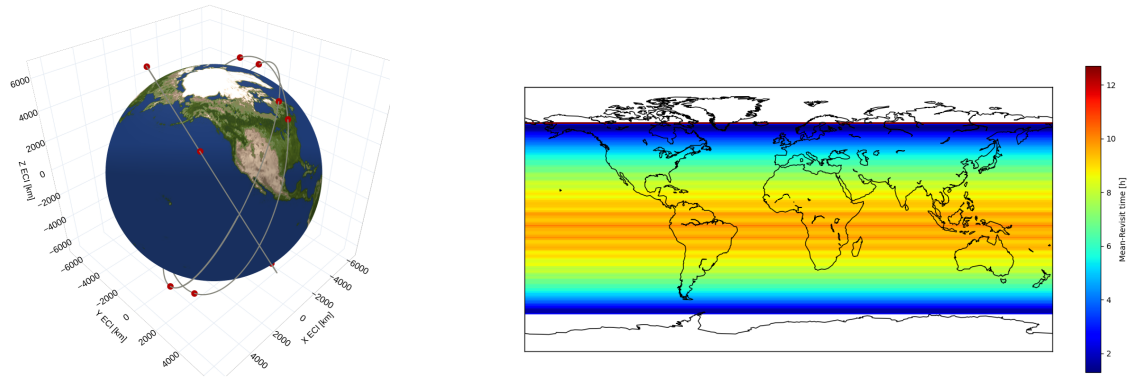

(c) GA-based configuration with 12 satellites.

Fig. 6 3D representations and mean revisit times of Walker, RGT, and GA-based configurations.

a desired pattern after deployment operations

Key areas for future developments of this promising constellation reconfiguration framework are the enhancement of maneuver cost estimation, including both time and fuel expenditure. Currently, the algorithm is able to estimate the low-thrust orbit transfer through literature-based estimates, but certain factors, such as the time of flight, phasing maneuvers, and precise fuel estimation with an electrical propulsion system, are not taken into account. Improving this aspect of the algorithm will enable a more accurate evaluation of the optimal configuration about the cost of the maneuvers required to reach the final configuration and will make the scenario more closely aligned with real scenarios.

References

[1] Paek, S. W., Kim, S., and de Weck, O., "Optimization of Reconfigurable Satellite Constellations Using Simulated Annealing and Genetic Algorithm," *Sensors*, Vol. 19, No. 4, 2019. https://doi.org/10.3390/s19040765, URL https://www.mdpi.com/1424-8220/19/4/765.

[2] Siddiqi, A., "Reconfigurability in space systems : architecting framework and case studies," Ph.D. thesis, Massachussets Institute of Technology, 2006.

[3] Scialom, U., "Optimization of satellite constellation reconfiguration," Ph.D. thesis, Massachusetts Institute of Technology, 2003.

[4] Davis, J., "Constellation Reconfiguration: Tools and Analysis," Ph.D. thesis, Texas A & M University, 2011.

[5] Ferringer, M. P., Spencer, D., and Reed, P., "Many-objective reconfiguration of operational satellite constellations with the Large-Cluster Epsilon Non-dominated Sorting Genetic Algorithm-II," *2009 IEEE Congress on Evolutionary Computation*, 2009, pp. 340–349.

[6] Paek, S., "Reconfigurable satellite constellations for geo-spatially adaptive Earth observation missions," Master's thesis, Massachussets Institute of Technology, 2012.

[7] Paganelli Azza, F., De Marchi, P., Stoisa, M., and Madonia, P. G., "Low-Thrust Reconfiguration Strategy for Flexible Satellite Constellations," 2022.

[8] Malkin, Z., "On subdivision of spherical surface into equal-area cells," *arXiv: Instrumentation and Methods for Astrophysics*, 2016.

[9] Larson, W. J., and Wertz, J. R., *Space mission analysis and design.*, Microcosm, 1992.

[10] Kenneally, P. W., Piggott, S., and Schaub, H., "Basilisk: A flexible, scalable and modular astrodynamics simulation framework," *Journal of aerospace information systems*, Vol. 17, No. 9, 2020, pp. 496–507.

[11] Tapley, B., Ries, J., Bettadpur, S., Chambers, D., Cheng, M., Condi, F., and Poole, S., "The GGM03 mean earth gravity model from GRACE," *AGU Fall Meeting Abstracts*, Vol. 2007, 2007, pp. G42A–03.

[12] Toronto-University, "Hypernova," , 2007. URL https://github.com/utat-ss/hypernova.

[13] Hoots, F. R., "An analytical satellite theory using gravity and a dynamic atmosphere," *AIAA paper*, 1982, pp. 81–1409.

[14] Hoots, F. R., "Jacchia-Linberry Atmo," *AIAA paper*, 1982, pp. 81–1409.

[15] Jah, M., Hughes, S., Wilkins, M., and Kelecy, T., "The general mission analysis tool (GMAT): A new resource for supporting debris orbit determination, tracking and analysis," *Proceedings of the Fifth European Conference on Space Debris*, 2009.

[16] Di Carlo, M., and Vasile, M., "Analytical solutions for low-thrust orbit transfers," *Celestial Mechanics and Dynamical Astronomy*, Vol. 133, No. 7, 2021, pp. 1–38.

[17] Zarrouati, O., *Trajectoires spatiales.*, 1987.

[18] Kramer, O., *Genetic Algorithms*, Springer International Publishing, Cham, 2017. https://doi.org/10.1007/978-3-319-52156-5_2, URL https://doi.org/10.1007/978-3-319-52156-5_2.

[19] Goldberg, D. E., *Genetic Algorithms in Search, Optimization and Machine Learning*, 1st ed., Addison-Wesley Longman Publishing Co., Inc., USA, 1989.

[20] Cantú-Paz, E., et al., "A survey of parallel genetic algorithms," *Calculateurs paralleles, reseaux et systems repartis*, Vol. 10, No. 2, 1998, pp. 141–171.

[21] Silberschatz, A., Gagne, G., and Galvin, P. B., *Operating System Concepts*, Wiley, 2002.

[22] Walker, J. G., "Satellite constellations," *Journal of the British Interplanetary Society*, Vol. 37, 1984, p. 559.